Chemical Science

EDGE ARTICLE

View Article Online
View Journal | View Issue

CrossMark click for updates

Cite this: *Chem. Sci.*, 2016, 7, 3025

A multi-dimensional quasi-zeolite with 12 × 10 × 7-ring channels demonstrates high thermal stability and good gas adsorption selectivity†

Jie Liang,[ab] Wei Xia,[c] Junliang Sun,*[ab] Jie Su,[b] Maofeng Dou,[d] Ruqiang Zou,[c] Fuhui Liao,[a] Yingxia Wang*[a] and Jianhua Lin[a]

Received 21st December 2015
Accepted 25th January 2016

DOI: 10.1039/c5sc04916d

www.rsc.org/chemicalscience

A novel quasi-zeolite PKU-15, with a rare 3-dimensional structure containing interconnected large (12-ring), medium (10-ring) and small (7-ring) multi-pore channels, was hydrothermally synthesised and characterised. A unique tri-bridging O^{2-} anion is found to be encapsulated in the cage-like $(Ge,Si)_{12}O_{31}$ building unit and energetically stabilises the PKU-15 framework. The removal of this oxygen atom would convert PKU-15 into a hypothetical zeolite PKU-15H. Thus, PKU-15 can be considered as a unique 'quasi-zeolite', which bridges porous germanates and zeolites. Owing to the absence of terminal Ge–OH groups in its structure, PKU-15 shows a remarkably high thermal stability of up to 600 °C. PKU-15 is also the first microporous germanate that exhibits permanent porosity, with a BET area of 428 $m^2\ g^{-1}$ and a good adsorption affinity toward CO_2.

Introduction

Zeolites, typically having a 3-dimensional (3D), 4-connected framework built from vertex-sharing TO_4 tetrahedra (T = Si, Al, Ge, *etc.*), are crystalline porous materials with well-defined pores of molecular dimensions. Owing to their tunable pore systems, these materials have been widely used in catalysis, gas sorption and separation, and ion-exchange.[1–9] Multi-pore zeolites with interconnected channels of different sizes are particularly important, as they allow the preferential diffusion of reactants and products through different channels when they are used as catalysts.[10–15] About 40 multi-pore zeolite frameworks have been found; however, only one of them (ITQ-22) has a 3D structure containing fully interconnected channels with small (8-ring), medium (10-ring), and large (12-ring) pores.[16] With this unique pore architecture, ITQ-22 shows a higher selectivity in the synthesis of ethylbenzene and cumene by the alkylation of benzene with ethanol and 2-propanol, respectively, as compared with ZSM-5 (10 × 10-ring) and beta zeolites (12 × 12 × 12-ring).[17] Thus, from the catalytic point of view, more zeolites with combined small, medium, and large pores are desirable.

The hydrothermal conditions for the synthesis of zeolites usually involve alkaline or nearly neutral fluoride medium. OH^- or F^-, acting as mineralizers, may be involved in the small building units, *e.g.* $[4^6]$, $[4^15^26^2]$, $[4^15^46^2]$, $[4^35^4]$, and $[4^35^26^1]$ cages, during the process.[18–24] Generally, these anions can be removed together with organic templates during calcination. But in some cases, the interactions between OH^-/F^- and the T atoms are so strong that these anions can become part of the framework as terminal groups and/or bridging species, for instance in the gallophosphate Mu-28,[25] the **AFR**-type aluminophosphate ($AlPO_4$-40),[26] the **SFO**-type aluminophosphate (SSZ-51)[27] and the **ZON**-type gallophosphate (DAB-2).[28] The effect of extra-framework anions encapsulated inside the small cages of the zeolite framework is substantial. On the one hand, these anions make their adjacent T atoms 5- or 6-coordinated, resulting in the porous compounds becoming 'quasi-zeolites'. On the other hand, theoretical calculations reveal that the inclusion of OH^- and F^- in the small building units may provide additional stabilisation energy for the formation of as-made zeolites.[29–31] Although the occlusion of OH^- or F^- anions in zeolite cages is common, little is known regarding the effect of O^{2-} anions encapsulated inside similar cages on the structures of zeolites. Herein we report the first example of a quasi-zeolite $|(CH_3)_3N(C_3H_7)|_2[Ge_{10.75}Si_{1.25}O_{19}O_{12/2}][Ge_3O_3O_{6/2}]$ (denoted as PKU-15) with a unique tri-bridging O^{2-} anion encapsulated within the cage-like $(Si,Ge)_{12}O_{31}$ building unit. The interaction between the trapped O^{2-} anion and the PKU-15 framework was also investigated by theoretical calculations. PKU-15 represents

[a]College of Chemistry and Molecular Engineering, Peking University, Beijing, 100871, China. E-mail: yxwang@pku.edu.cn; junliang.sun@pku.edu.cn

[b]Berzelii Center EXSELENT on Porous Materials and Inorganic and Structural Chemistry, Department of Materials and Environmental Chemistry, Stockholm University, Stockholm, 10691, Sweden

[c]College of Engineering, Peking University, Beijing, 100871, China

[d]Department of Materials Science and Engineering, Royal Institute of Technology, Stockholm, 10044, Sweden

† Electronic supplementary information (ESI) available: Synthesis, detailed structure description, structure refinement, NMR spectra, and CIFs. CCDC 1059012. For ESI and crystallographic data in CIF or other electronic format see DOI: 10.1039/c5sc04916d

a unique fully interconnected multi-pore system with large (12-ring), medium (10-ring), and small (7-ring) channels. Its thermal stability and gas adsorption properties were also investigated.

Results and discussion

PKU-15 was hydrothermally synthesised by using trimethylpropylammonium hydroxide ($Me_3PrN^+OH^-$) as the structure-directing agent (SDA). A single crystal with the size 280 × 40 × 20 μm^3 was selected for X-ray diffraction studies (Fig. S1†). The phase purity was confirmed by the agreement between the experimental powder X-ray diffraction pattern and the simulated one based on the single crystal X-ray diffraction results (Fig. S2†).

PKU-15 crystallizes in the orthorhombic space group *Pnma* (no. 62) with the lattice constants a = 16.8108(5) Å, b = 19.7138(7) Å and c = 23.9394(9) Å. The framework is built from a novel $(Ge,Si)_{12}O_{31}$ cluster and Ge_3O_9 3-ring units. The 3-ring unit is rare in silicates, but is relatively common in germanates due to the favourable bond parameters of [GeO_4] units.[32] The $(Ge,Si)_{12}O_{31}$ cluster, consisting of three GeO_5 trigonal bipyramids and nine $(Ge,Si)O_4$ tetrahedra, is a novel building unit (BU) which has never been reported before (Fig. 1a). In each $(Ge,Si)_{12}O_{31}$ cluster, an oxygen anion is encapsulated within the BU and linked to three Ge atoms (Ge1, Ge2 and Ge3), making them 5- rather than 4-coordinated, with a trigonal bipyramidal geometry. This produces a Ge_3O_7 trimer in the centre of the cluster (Fig. 1b). Nine $(Ge,Si)O_4$ tetrahedra are then connected to the trimer through corner-sharing oxygen atoms, giving rise to the non-centrosymmetric $(Ge,Si)_{12}O_{31}$ cluster [simplified as $(Ge,Si)_{12}$ hereafter].

The PKU-15 framework can be described as $(Ge,Si)_{12}O_{25}$ layers interconnected by Ge_3O_9 3-rings (Fig. 2). The $(Ge,Si)_{12}O_{25}$ layer is formed solely by $(Ge,Si)_{12}$ clusters, where one $(Ge,Si)_{12}$ cluster connects to two neighbouring clusters by sharing a pair of oxygen vertices along the *a*-axis, and to another two clusters by sharing one corner of the tetrahedron along the *b*-axis. Such

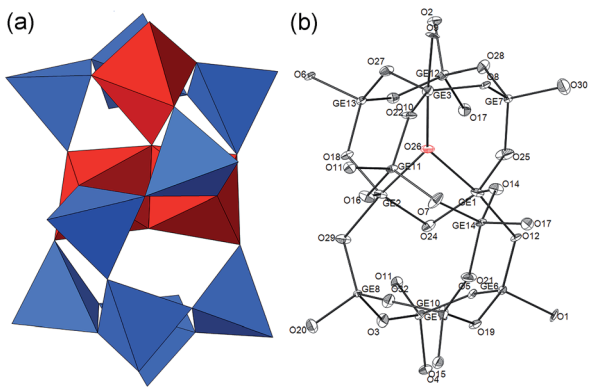

Fig. 1 $(Ge,Si)_{12}O_{31}$ cluster in PKU-15. (a) Polyhedral and (b) thermal ellipsoidal (50%) representations of the cluster. In (a), the GeO_5 trigonal bipyramids are drawn in red, and the GeO_4 tetrahedra are in blue. In (b), the tri-coordinated oxygen atom in the cluster is drawn in red.

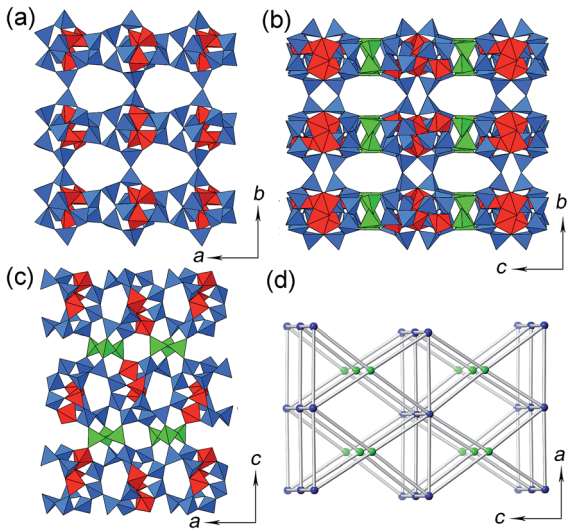

Fig. 2 Framework of PKU-15. Polyhedral representations of PKU-15 viewed along the (a) *c*-, (b) *a*- and (c) *b*-axis. (d) Concise topology showing the linkage of $(Ge,Si)_{12}$ clusters and Ge_3O_9 3-rings. In (a)–(c), the GeO_5 trigonal bipyramids and $(Ge,Si)O_4$ tetrahedra in the $(Ge,Si)_{12}$ clusters are shown in red and blue, respectively, while the Ge_3O_9 3-ring units are drawn in green. In (d), the $(Ge,Si)_{12}O_{31}$ clusters and Ge_3O_9 3-rings are simplified as blue and green solid balls, respectively, showing their connectivity.

a connection gives rise to the $(Ge,Si)_{12}O_{25}$ layer with elliptical 10-ring holes in the *ab*-plane (Fig. 2a). Neighbouring $(Ge,Si)_{12}O_{25}$ layers, related by an *a*-glide normal to the *c*-axis, are then linked *via* Ge_3O_9 3-rings, forming the 3D framework of PKU-15 (Fig. 2b and c). The PKU-15 framework can be sketched as a 4,8-heterocoordinated sqc21 net (Fig. 2d), in which the $(Ge,Si)_{12}$ cluster shares all its 12 corners and acts as an 8-linkage node, and the Ge_3O_9 3-ring acts as a 4-linkage knot. This also results in a 3D interconnected channel system in PKU-15. A 12-ring sinusoidal channel with an opening of 3.7 Å × 8.7 Å runs along the *a*-axis, a 7-ring (2.3 Å × 4.0 Å) channel runs along the *b*-axis, and a 10-ring channel (4.0 Å × 6.1 Å) runs along the *c*-axis, assuming that the van der Waals radius is 1.35 Å for oxygen (Fig. S3 and S4†). Note that, unlike the circular 12-ring pores in other zeolite frameworks, the 12-ring pore window in PKU-15 is rather squashed. This, combined with the unique 3D 12 × 10 × 7-ring multi-pore channel system, makes PKU-15 a potential catalyst candidate in the petrochemical industry.

The most interesting structural feature of PKU-15 is the presence of the tri-coordinated oxygen atom (O26) within the cage-like $(Ge,Si)_{12}$ cluster. The removal of O26 could transform PKU-15 into a hypothetical zeolite framework (denoted as PKU-15H), and the $(Ge,Si)_{12}$ cluster could be described by a hypothetical zeolitic -4-4-4- BU, which is transformed from the known 4-4- BU by inserting a third 4-ring in the middle (Fig. 3a and b). The structure of PKU-15H can be illustrated with the aid of the **ZON** framework, which is solely built from the 4-4-BU.[28,33–36] Similar to the connection mode of the 4-4- BU in **ZON**, neighbouring -4-4-4- BUs in the PKU-15H framework are joined in a 'head to tail' fashion to form chains running parallel to the *a*-axis (Fig. 3c and e). The adjacent chains, related by inversion

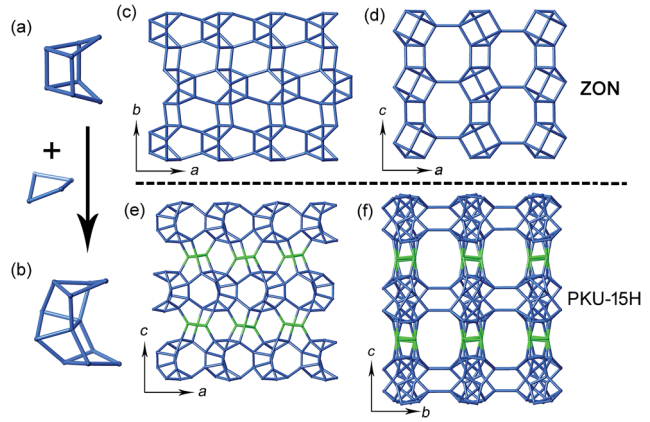

Fig. 3 Relationship between the **ZON** framework and the hypothetical zeolite PKU-15H. (a) The 4-4- BU in the **ZON** framework. (b) The -4-4-4- BU in PKU-15H. (c) and (d) are the structural projections of the **ZON** framework viewed along the *c*- and *b*-axes, respectively. (e) and (f) are the projections of the hypothetical zeolite PKU-15H viewed along the *b*- and *a*-axes, respectively. In (e) and (f), the Ge_3O_9 3-rings are drawn in green. All of the oxygen atoms in the two frameworks are omitted for clarity.

symmetry, are linked directly in the **ZON** framework (Fig. 3c), whereas they are crosslinked *via* Ge_3O_9 3-rings in PKU-15H (Fig. 3e). The involvement of the Ge_3O_9 3-rings endows PKU-15H with a larger sinusoidal 12-ring channel along the *a*-axis (Fig. 3f), as compared with the sinusoidal 8-ring channel in the **ZON** framework (Fig. 3d). It is worth noting that in the aluminophosphate analogue of **ZON** (UiO-7), a similar di-bridging fluoride anion is observed within the cage-like 4-4- BU.[35] However, in the zinco-aluminophosphate analogue of **ZON** (ZAPO-M1), no similar bridging position is found.[33] This hints that, by introducing negative charges in the framework, such as substituting Ge^{4+} with Al^{3+}, the tri-bridging oxygen anion may be removed from the framework and realize the transformation from PKU-15 into PKU-15H. Related work is being studied.

As mentioned above, the tri-coordinated oxygen atom makes PKU-15 a quasi-zeolite. To further understand its role in the formation of the PKU-15 framework, we performed total energy calculations for PKU-15 and PKU-15H based on first-principles.[36,37] The two systems were set in the same unit cell, and the only difference is the absence of the tri-coordinated O26 atom in PKU-15H (see Experimental section). To investigate the role that other anions, such as F^-, played in the framework formation, similar calculations were also performed for UiO-7 and UiO-7 without the di-bridging F atom (denoted as UiO-7H).[35] As expected, the calculated energies for PKU-15 and UiO-7 are about 3.77 eV and 2.2 eV lower than those for PKU-15H and UiO-7H, respectively, suggesting that the extra-framework anions (O^{2-} and F^-) do provide additional stabilisation for the frameworks. The much larger energy difference in the PKU-15 system than in the UiO-7 system may suggest that the O^{2-} anion is more crucial for the formation of PKU-15 than the F^- anion for the formation of UiO-7. Thus, it may be more difficult to release O^{2-} anions from the cages, as compared with the F^- species. As indicated in the literature, the F^- anions in UiO-7 can be removed by calcination at approximately 450–550 °C;[35] however, in our calculations, the O^{2-} anions can only escape from the -4-4-4- cages in PKU-15 when the heating temperature reaches 1000 °C. Since the PKU-15 framework will collapse at 600 °C due to the breaking of other Ge–O bonds, we cannot obtain the PKU-15 framework without the tri-coordinated O26 atom by direct heating.

Except for the tri-coordinated O26 atom, all the other oxygen atoms in PKU-15 are shared by two neighbouring germanium atoms; thus, there is no terminal group in the PKU-15 framework. As is known, –OH terminal groups are a common feature of porous germanates and can induce a condensation process which may cause the collapse of the framework during heating.[38,39] Thus, it is expected that the absence of terminal –OH groups may endow PKU-15 with a high thermal stability. This is proved by TG analysis and *in situ* variable-temperature powder X-ray diffraction (Fig. 4). In the TG curve, the weight loss of 11.7 wt% (calcd 11.8 wt%) in the range between 200 °C and 700 °C is attributed to the removal of organic templates (Fig. 4a). A main endothermic peak at approximately 450 °C is also observed in the DSC curve, owing to SDA removal (Fig. 4a). As evidenced by the *in situ* variable-temperature powder X-ray diffraction data, PKU-15 retains its framework integrity up to about 600 °C, even after guest removal (Fig. 4b). The thermal stability of PKU-15 is among the highest reported for porous germanates, and is even

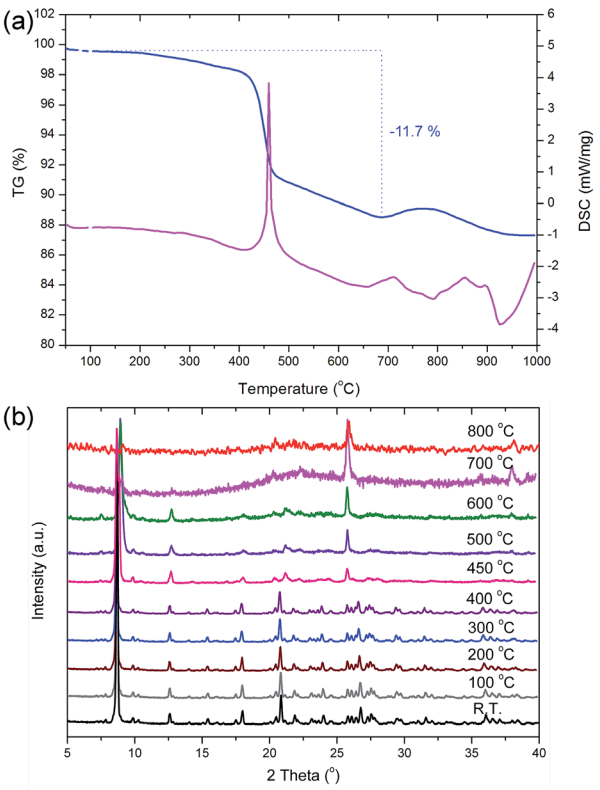

Fig. 4 The thermal properties of as-synthesised PKU-15. (a) TG-DSC curves of as-synthesised PKU-15. The TG curve is drawn in blue, and the DSC curve is in purple. (b) *In situ* variable-temperature powder X-ray diffraction patterns of as-synthesised PKU-15 heated from room temperature (R.T.) to 800 °C.

higher than some germanate-based zeolites, such as SU-16,[40] PKU-9,[41] GaGe-JU-64,[42] and PKU-14.[43]

Four half-occupied $[(CH_3)_3N(C_3H_7)]^+$ (shortened to Me_3PrN^+) cations are located in the 12- and 10-ring channels to compensate the −2 charge of the PKU-15 framework (Fig. S5†). Unlike other germanates that usually undergo structure collapse during the removal of organic species, the Me_3PrN^+ cations in PKU-15 can be totally removed while keeping the framework integrity after heating in ozone for 6 hours (Fig. S6†). Thus, the porosity of the germanate-based PKU-15 quasi-zeolite can be characterised. The N_2 sorption isotherms of the ozone-treated sample at 77 K exhibit a typical type-I behavior, indicating the microporous features of PKU-15 (Fig. 5a). The BET area is 428 $m^2\ g^{-1}$, compared with about 750 $m^2\ g^{-1}$ for a silicate analogue. At 273 K, the ozone-treated PKU-15 sample can adsorb a large amount of CO_2 (1.0 mmol g^{-1}, 22.6 $cm^3\ g^{-1}$) at 1.0 bar (Fig. 5b). This value is lower than that of the 'benchmark' 13X zeolite (7.06 mmol g^{-1}),[44] but is higher than that of our recently reported mesoporous germanate PKU-17 (0.7 mmol g^{-1}).[45] In light of the unique channel system in PKU-15, we further tested its selective gas adsorption properties. In addition to the CO_2 adsorption measurements, CH_4, C_2H_4, C_2H_6 and N_2 adsorption studies were also carried out at 273 K. As expected, PKU-15 can adsorb a moderate amount of CH_4 (0.5 mmol g^{-1}, 11.3 $cm^3\ g^{-1}$), slightly lower amounts of C_2H_4 (0.32 mmol g^{-1}, 7.3 $cm^3\ g^{-1}$) and N_2 (0.28 mmol g^{-1}, 6.3 $cm^3\ g^{-1}$), and a limited amount of C_2H_6 (0.18 mmol g^{-1}, 4.2 $cm^3\ g^{-1}$). In view of the kinetic diameters of 3.3 Å for CO_2, 3.6 Å for CH_4, 3.8 Å for N_2, 4.2 Å for C_2H_4, and 4.4 Å for C_2H_6, it can be inferred that the pore openings in PKU-15 should be approximately 3.8–4.2 Å in diameter. This is consistent with the crystallographically observed aperture size of 3.7 Å × 8.7 Å for PKU-15. The adsorption selectivity for CO_2 over other gases shown by PKU-15 may have applications in the separation of CO_2 from flue-gas streams and the separation of CO_2 from hydrocarbons.

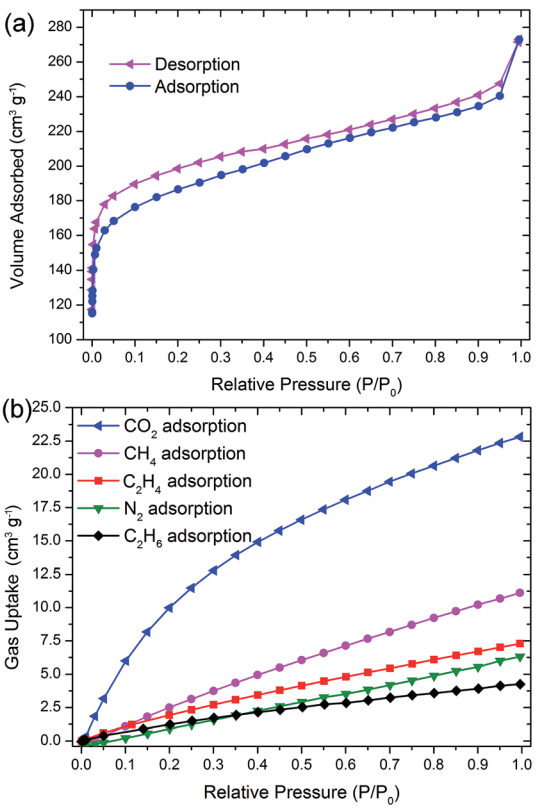

Fig. 5 Gas sorption isotherms of ozone-treated PKU-15. (a) N_2 sorption isotherms at 77 K. (b) CO_2, CH_4, C_2H_4, N_2 and C_2H_6 adsorption isotherms at 273 K. P_0 represents the standard pressure.

Conclusions

In summary, a novel silicogermanate quasi-zeolite PKU-15 with 3D 12 × 10 × 7-ring multi-pore channels was synthesised by using $Me_3PrN^+OH^-$ as the SDA. The framework of PKU-15 is built from two BUs, the known Ge_3O_9 3-ring unit and a new $(Ge,Si)_{12}O_{31}$ cluster, which are arranged in a 4,8-heterocoordinated sqc21 net. Without any terminal –OH groups, PKU-15 shows a high thermal stability of up to 600 °C. It also shows a good affinity towards CO_2. For the first time, a tri-coordinated oxygen anion is found to be encapsulated in the cage-like $(Ge,Si)_{12}O_{31}$ cluster and provides a high additional stabilisation energy for the framework. The successful removal of the O^{2-} anion would transform PKU-15 into a hypothetical zeolite PKU-15H. Thus, the discovery of the quasi-zeolite PKU-15 may build a bridge between porous germanates and zeolites.

Experimental section

Synthesis

Certain amounts of amorphous SiO_2 and GeO_2 were mixed with $Me_3PrN^+OH^-$ solution, and the mixture was stirred until a uniform suspension was formed. The composition of the initial gel was $0.1SiO_2 : 0.9GeO_2 : 0.5Me_3PrN^+OH^- : xH_2O$, $x = 3$–7. The mixture was transferred into a Teflon-lined stainless steel autoclave and heated at 175 °C for 14 days. The colourless single crystals were filtered, washed with ethanol, and then dried at 60 °C overnight. The sample was calcined at 200 °C in O_3 for 6 hours to remove the organic species in the channels.

Structure determination

A suitable single crystal of PKU-15 with dimensions of 280 × 40 × 20 μm^3 was selected for single crystal X-ray diffraction measurements. Data were collected on a Supernova diffractometer with graphite-monochromated MoKα radiation (λ = 0.71073 Å) at 100 K. Data reduction and numerical absorption correction were applied using CrysAlisPro. The structure was solved by using direct methods and refined on F^2 using the full-matrix least-squares technique with the SHELX program.[46,47] The structure of PKU-15 is orthorhombic and contains 15 unique T (T = Ge, Si) atoms in an asymmetric unit. The three 5-coordinated T-atoms and the three 4-coordinated T-atoms related to the 3-rings were refined as Ge atoms. After one round, the T atom with a Ge occupancy of more than 1.0 was also refined as Ge. In the remaining eight 4-coordinated positions, Ge and Si were randomly distributed with occupancies ranging

from 0.849 to 0.982 for Ge and 0.018 to 0.151 for Si. All non-hydrogen atom positions except carbon were refined anisotropically. The carbon chains were refined with restraints, by fixing the C–C and N–C distances. Hydrogen atoms in the SDA were introduced in the ideal positions as riding on their bonded atoms and were assigned isotropic thermal parameters 1.2 and 1.5 times those of the bonded C atoms. The crystallographic data and structure refinement results are summarised in Table S1.† CCDC 1059012 contains the supplementary crystallographic data for this paper.

Computing method

Our first-principles calculations were carried out with density functional theory (DFT) as implemented in the Vienna *Ab Initio* Simulation Package (VASP).[48,49] The calculations were performed based on the projector augmented wave (PAW) method with plane-wave cutoff energy of 400 eV.[36,37] The exchange–correlation potential was described using Perdew–Burke–Ernzerhof (PBE).[50] The Brillouin-zone integration was performed with a $2 \times 2 \times 2$ Monkhorst–Pack *k*-mesh. Owing to the large numbers of atoms and to reduce calculation time, the internal atomic coordinates were fixed. Considering one less O atom in PKU-15H than in PKU-15, the energy difference between PKU-15 and PKU-15H was calculated based on:

$$\Delta E = E^{\mathrm{tot}}_{\text{PKU-15}} - E^{\mathrm{tot}}_{\text{PKU-15H}} - \frac{1}{2}E^{\mathrm{tot}}_{\mathrm{O_2}}$$

where $E^{\mathrm{tot}}_{\text{PKU-15}}$, $E^{\mathrm{tot}}_{\text{PKU-15H}}$ and $E^{\mathrm{tot}}_{\mathrm{O_2}}$ are the total energies of PKU-15, PKU-15H and the O_2 molecule, respectively. The non-configurational entropy and electron entropy were not considered in this calculation.

Acknowledgements

This work was financially supported by the National Natural Science Foundation of China (21171009, 11275012, 21471009 and 21321001) and the State Science and Technology Commission of China (2012CB224802 and 2013CB933402). The author thanks Xiaohuan Lin, Hao Zhang, Yanping Chen and Youyou Yuan for helpful discussions.

References

1 D. W. Breck, *Zeolite Molecular Sieves: Structure, Chemistry, and Use*, Wiley, New York, 1974.
2 R. M. Barrer, *Hydrothermal Chemistry of Zeolite*, Academic Press, London, 1982.
3 J. V. Smith, *Chem. Rev.*, 1988, **88**, 149–182.
4 A. Corma, *Chem. Rev.*, 1995, **95**, 559–614.
5 C. S. Cundy and P. A. Cox, *Chem. Rev.*, 2003, **103**, 663–701.
6 Y. Li and J. Yu, *Chem. Rev.*, 2014, **114**, 7268–7316.
7 J. Li, A. Corma and J. Yu, *Chem. Soc. Rev.*, 2015, **44**, 7112–7127.
8 B. M. Weckhuysen and J. Yu, *Chem. Soc. Rev.*, 2015, **44**, 7022–7024.
9 P. Guo, J. Shin, A. G. Greenaway, J. G. Min, J. Su, H. J. Choi, L. Liu, P. A. Cox, S. B. Hong, P. A. Wright and X. Zou, *Nature*, 2015, **524**, 74–78.
10 E. G. Derouane and Z. Gabelica, *J. Catal.*, 1980, **65**, 486.
11 M. Moliner, C. Martínez and A. Corma, *Angew. Chem., Int. Ed.*, 2015, **54**, 3560–3579.
12 M. Moliner, J. González, M. T. Portilla, T. Willhammar, F. Rey, F. J. Llopis, X. Zou and A. Corma, *J. Am. Chem. Soc.*, 2011, **133**, 9497–9505.
13 T. Willhammar, J. Sun, W. Wan, P. Oleynikov, D. Zhang, X. Zou, M. Moliner, J. Gonzalez, C. Martínez, F. Rey and A. Corma, *Nat. Chem.*, 2012, **4**, 188–194.
14 J. Jiang, Y. Yun, X. Zou, J. L. Jorda and A. Corma, *Chem. Sci.*, 2015, **6**, 480–485.
15 W. Hua, H. Chen, Z. Yu, X. Zou, J. Lin and J. Sun, *Angew. Chem., Int. Ed.*, 2014, **53**, 5868–5871.
16 A. Corma, F. Rey, S. Valencia, J. L. Jorda and J. Rius, *Nat. Mater.*, 2003, **2**, 493–497.
17 A. Corma, F. J. Llopis, C. Martinez, G. Sastre and S. Valencia, *J. Catal.*, 2009, **268**, 9–17.
18 A. Corma, M. J. Díaz-Cabañas, J. Martínez-Triguero, F. Rey and J. Rius, *Nature*, 2002, **418**, 514–517.
19 P. Caullet, J. L. Guth, J. Hazm, J. M. Lamblin and H. Gies, *Eur. J. Solid State Inorg. Chem.*, 1991, **28**, 345–361.
20 Y. Wang, J. Song and H. Gies, *Solid State Sci.*, 2003, **5**, 1421–1433.
21 B. F. Mentzen, M. Sacerdote-Peronnt, J. L. Guth and H. Kessler, *C. R. Acad. Paris. Ser. II*, 1991, **313**, 177–182.
22 G. Van de Goor, C. C. Freyhardt and P. Behrens, *Z. Anorg. Allg. Chem.*, 1995, **621**, 311–322.
23 M. A. Camblor, M. J. Díaz-Cabañas, J. Perez-Pariente, S. J. Teat, W. Clegg, I. J. Shannon, P. Lightfoot, P. A. Wright and R. E. Morris, *Angew. Chem., Int. Ed.*, 1998, **37**, 2122–2162.
24 P. A. Barrett, M. A. Camblor, A. Corma, R. H. Jones and L. A. Villaescua, *J. Phys. Chem. B*, 1998, **102**, 4147–4155.
25 L. Josien, A. Simon-Masseron, V. Gramlich, F. Porcher and J. Patarin, *J. Solid State Chem.*, 2004, **177**, 3721–3728.
26 V. Ramaswamy, L. B. McCusker and C. Baerlocher, *Microporous Mesoporous Mater.*, 1999, **31**, 1–8.
27 R. E. Morris, A. Burton, L. M. Bull and S. I. Zones, *Chem. Mater.*, 2004, **16**, 2844–2851.
28 A. Meden, R. W. Grosse-Kunstleve, C. Baerlocher and L. B. McCusker, *Z. Kristallogr.*, 1997, **212**, 801–807.
29 A. R. George and C. R. A. Catlow, *Chem. Phys. Lett.*, 1995, **247**, 408–417.
30 M. A. Camblor, L. A. Villaescusa and M. J. Díaz-Cabañas, *Top. Catal.*, 1999, **9**, 59–76.
31 A. R. George and C. R. A. Catlow, *Zeolites*, 1997, **18**, 67–70.
32 C. Baerlocher, L. B. McCusker and D. H. Olson, *Atlas of Zeolite Framework Types*, Elsevier, New York, 6th edn, 2007.
33 B. Marler, J. Patarin and L. Sierra, *Microporous Mater.*, 1995, **5**, 151–159.
34 D. E. Akporiaye, H. Fjellvag, E. N. Halvorsen, J. Hustveit, A. Karlsson and K. P. Lillerud, *Chem. Commun.*, 1996, 601–602.

35 D. E. Akporiaye, H. Fjellvåg, E. N. Halvorsen, J. Hustveit, A. Karlsson and K. P. Lillerud, *J. Phys. Chem.*, 1996, **100**, 16641–16646.
36 G. Kresse and D. Joubert, *Phys. Rev. B: Condens. Matter*, 1999, **59**, 1758–1775.
37 P. E. Blöchl, *Phys. Rev. B: Condens. Matter*, 1994, **50**, 17953–17979.
38 M. Davis, *Nature*, 2002, **417**, 813–821.
39 Y. Xu, L. Cheng and L. W. You, *Inorg. Chem.*, 2006, **45**, 7705–7708.
40 Y. Li and X. Zou, *Angew. Chem., Int. Ed.*, 2005, **44**, 2012–2015.
41 J. Su, Y. Wang, Z. Wang and J. Lin, *J. Am. Chem. Soc.*, 2009, **131**, 6080–6081.
42 Y. Xu, Y. Li, Y. Han, X. Song and J. Yu, *Angew. Chem., Int. Ed.*, 2013, **52**, 5501–5503.
43 J. Liang, J. Su, Y. Wang, Y. Chen, X. Zou, F. Liao, J. Lin and J. Sun, *Chem. – Eur. J.*, 2014, **20**, 16097–16101.
44 P. Aprea, D. Caputo, N. Gargiulo, F. Lucolano and F. Pape, *J. Chem. Eng. Data*, 2010, **55**, 3655–3661.
45 J. Liang, J. Su, X. Luo, Y. Wang, H. Zheng, H. Chen, X. Zou, J. Lin and J. Sun, *Angew. Chem., Int. Ed.*, 2015, **54**, 7290–7294.
46 G. M. Sheldrick, *Program for solution of crystal structures*, University of Göttingen, 1997.
47 G. M. Sheldrick, *Acta Crystallogr., Sect. A: Found. Crystallogr.*, 2008, **64**, 112–122.
48 G. Kresse and J. Hafner, *Phys. Rev. B: Condens. Matter*, 1993, **47**, 558–561.
49 G. Kresse and J. Furthmüller, *Phys. Rev. B: Condens. Matter*, 1996, **54**, 11169–11186.
50 J. P. Perdew, K. Burke and M. Ernzerhof, *Phys. Rev. Lett.*, 1996, **77**, 3865–3868.